References

Bank, H., Henn, U. & Milisenda, C.C. 1998. Anorthit aus Japan. *Gemmologie: Zeitschrift der Deutschen Gemmologischen Gesellschaft*, **47**, 62–63.

Deer, W.A., Howie, R.A. & Zussman, J. 1992. *An Introduction to the Rock-Forming Minerals*. 2nd edn. Longman Scientific & Technical, Harlow, Essex, 696 pp.

Kikuchi, Y. 1888. On anorthite from Miyakejima. *Journal of the College of Science, Imperial University of Tokyo*, **2**(1), 31–47.

Murakami, H., Kimata, M. & Shimoda, S. 1991. Native copper included by anorthite from the island of Miyakejima: Implications for arc magmatism. *Journal of Mineralogy, Petrology and Economic Geology*, **86**(8), 364–374, http://doi.org/10.2465/ganko.86.364.

Aquamarine from Southern Ethiopia: An Update

Figure 2: These beryls, seen during the February 2019 Tucson gem shows, are reportedly from southern Ethiopia. The largest crystal weighs 613.4 g. Photo by T. Sripoonjan.

During the February 2019 Tucson gem shows, author TS encountered some beryl crystals that were reportedly from the Shakiso region of southern Ethiopia (Figure 2). Some of them consisted of aquamarine, showing apparently hexagonal prism faces, which were relatively larger in size (up to 600+ g) than previously reported by Laurs (2012) and Laurs *et al.* (2014). The vendors, Arjit and Apurva Birani (Plum Colors, Bangkok, Thailand), informed the author that the beryl came from a recent discovery that occurred near the Shakiso emerald deposit. In addition to the rough material, they also had faceted stones, although these had all sold before the author visited their booth.

Recently, at the Plum Colors office in Bangkok, these authors saw some more of the Ethiopian aquamarine. One of the faceted stones was an attractive, consistent blue with high clarity (Figure 3). Author TS borrowed

Figure 3: This 8.16 ct Ethiopian aquamarine was recently cut in Bangkok and shows an attractive blue colour. Photo by T. Sripoonjan.

Figure 4: (**a**) Etch pits of various shapes decorate the prism face of an Ethiopian aquamarine crystal (reflected light, image width 10.0 mm). (**b**) Thin films displaying iridescent colours are arranged in planes perpendicular to the c-axis of the aquamarine (reflected light, image width 2.0 mm). (**c**) The only internal features that were visible in the faceted Ethiopian aquamarine in Figure 3 are these growth lines (darkfield illumination, image width 5.2 mm). Photomicrographs by T. Sripoonjan.

this gem and six rough samples for examination. The faceted stone weighed 8.16 ct (16.32 × 8.97 × 7.47 mm) and the rough ranged from 2.3 to 16.3 g. The samples were greenish blue to pure medium blue and showed strong pleochroism in near-colourless and blue. The RIs were 1.570–1.582 (birefringence 0.012) and the hydrostatic SG averaged 2.66. The samples were inert to both long- and short-wave UV radiation.

The aquamarine crystals exhibited obvious etch pits of various shapes on their prism faces (Figure 4a). Internal features in the rough material consisted of a complex network of parallel partially healed fissure planes, two-phase fluid inclusions, colourless mineral inclusions (0.1–0.5 mm) and especially multiple planes of thin films showing iridescence (Figure 4b). However, the faceted stone solely contained growth lines (Figure 4c).

Raman spectroscopy with a Renishaw inVia unit confirmed that the stones were beryl (aquamarine). Polarised ultraviolet-visible-near infrared (UV-Vis-NIR) spectroscopy of the faceted stone revealed two sharp peaks at 370 and 427 nm related to Fe^{3+} and a strong, broad absorption band centred at ~820 nm due to Fe^{2+} (Figure 5a). Two sidebands at ~620 and 955 nm have been attributed to Fe^{2+} intervalence charge transfer (Burns 1993). The Fe-related absorptions formed a transition window at around 480–530 nm that accounts for blue colouration in aquamarine. A peak at 1147 nm has yet to be assigned, and there were essentially no distinct absorption features in the visible region of the spectra.

Mid-infrared spectroscopy of all samples using a Thermo Scientific Nicolet 6700 FTIR spectrometer yielded consistent features in the 7400–4500 cm^{-1} region (e.g. Figure 5b). A band at around 7140 cm^{-1} was more intense than the adjacent features at 7098 and 7075 cm^{-1}. This correlates to a prevalence of type I H_2O associated with very low alkali contents in this aquamarine (cf. Saeseaw *et al.* 2014).

Energy-dispersive X-ray fluorescence (EDXRF) spectroscopy of all samples with a Thermo Scientific ARL Quant'X instrument showed distinct amounts of iron (0.40–1.40 wt.% Fe_2O_3), although substantially less than in some aquamarine reported in the literature (e.g. Canada, Adamo *et al.* 2008; Vietnam, Huong *et al.* 2011). In addition, these

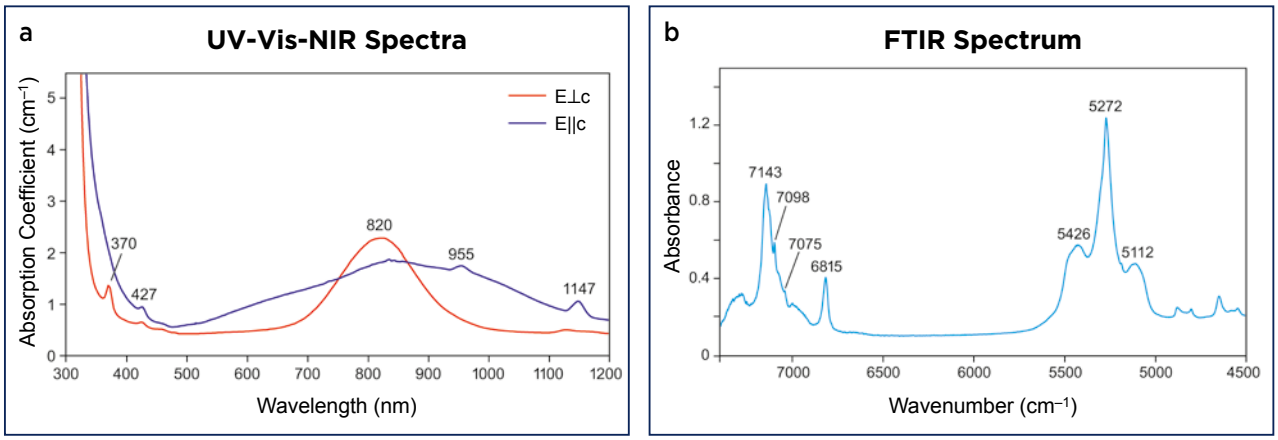

Figure 5: (**a**) Polarised UV-Vis-NIR spectra of the faceted Ethiopian aquamarine in Figure 3 show features mainly associated with iron. The path length of the beam through the sample was 7.47 mm. (**b**) A representative FTIR spectrum of the Ethiopian aquamarine reveals several bands related to type I and type II H_2O, with the former being more prevalent.

Ethiopian aquamarines were characterised by relatively high concentrations of potassium (up to 0.24 wt.% K_2O). Caesium contents were very low (averaging 0.03 wt.% Cs_2O) compared to those of aquamarine from other sources (Bocchio *et al.* 2009; Huong *et al.* 2011).

Previous articles (Laurs 2012; Laurs *et al.* 2014) supplied brief information on Ethiopian aquamarine, and this report provides additional data that may be helpful to gemmologists in case this material becomes more common in the marketplace in the future.

Tasnara Sripoonjan (stasnara@git.or.th) and
Dr Montira Seneewong Na Ayutthaya
Gem and Jewelry Institute of Thailand, Bangkok

References

Adamo, I., Pavese, A., Prosperi, L., Diella, V., Ajò, D., Gatta, G.D. & Smith, C.P. 2008. Aquamarine, Maxixe-type beryl, and hydrothermal synthetic blue beryl: Analysis and identification. *Gems & Gemology*, **44**(3), 214–226, http://doi.org/10.5741/gems.44.3.214.

Bocchio, R., Adamo, I. & Caucia, F. 2009. Aquamarine from the Masino-Bregaglia massif, central Alps, Italy. *Gems & Gemology*, **45**(3), 204–207, http://doi.org/10.5741/gems.45.3.204.

Burns, R.G., 1993. *Mineralogical Applications of Crystal Field Theory*. 2nd edn. Cambridge University Press, Cambridge, 576 pp.

Huong, L.T.-T., Hofmeister, W., Häger, T., Khoi, N.N., Nhung, N.T., Atichat, W. & Pisutha-Arnond, V. 2011. Aquamarine from the Thuong Xuan District, Thanh Hoa Province, Vietnam. *Gems & Gemology*, **47**(1), 42–48, http://doi.org/10.5741/gems.47.1.42.

Laurs, B.M. 2014. Gem Notes: Prismatic aquamarine crystals from Ethiopia. *Journal of Gemmology*, **34**(1), 8–9.

Laurs, B.M., Simmons, W.B. & Falster, A.U. 2012. Gem News International: New gem discoveries in Ethiopia. *Gems & Gemology*, **48**(1), 66–67.

Saeseaw, S., Pardieu, V. & Sangsawong, S. 2014. Three-phase inclusions in emerald and their impact on origin determination. *Gems & Gemology*, **50**(2), 114–132, http://doi.org/10.5741/gems.50.2.114.

Chrysocolla from the Ray Mine, Arizona, USA

For decades, the Ray mine near Kearny, Pinal County, Arizona, USA, has been a well-known source of copper minerals that are prized by collectors (e.g. Jones & Wilson 1983). The copper ore at this porphyry copper deposit was naturally concentrated by secondary enrichment processes, resulting in the formation of abundant chrysocolla and other secondary copper minerals. Chrysocolla has been mined as bright blue-to-green masses, vug fillings, stalactites and pseudomorphs. The mine is still being exploited for copper, and occasionally small amounts of high-quality chrysocolla specimens, gem rough and polished stones appear on the market, such as those seen by this author at the February 2019 Pueblo Gem & Mineral Show in Tucson (e.g. Figure 6). In addition to mineral specimens, there were approximately 50 cabochons that had been cut from ~3 kg of rough material produced in 2018. The largest cabochon measured 30.5 × 18.5 mm, and the chrysocolla was translucent to semi-transparent with an attractive blue to bluish green colour that was evenly distributed in most of the polished pieces.

Figure 6: This rough specimen (68.0 mm long) and cabochon of chrysocolla were recently produced from the Ray mine in Arizona. Shown for comparison is a carving (27.4 mm long) made from high-quality chrysocolla that is from elsewhere in Arizona. The rough specimen is covered by drusy quartz, and the greener portion may correspond to the presence of malachite. Photo by B. M. Laurs.

Although chrysocolla from the Ray mine is seldom seen on the market today, occasionally high-quality material is encountered, as shown by the examples documented here.

Brendan M. Laurs FGA

Reference

Jones, R.W. & Wilson, W.E. 1983. Famous mineral localities: The Ray mine. *Mineralogical Record*, **14**(5), 311–322.